Concentration and temperature dependence of decomposition in supercooled liquid alloys

Jörg F. Löffler,[a*] P. Thiyagarajan [b] and William L. Johnson [a]

[a]*California Institute of Technology, W. M. Keck Laboratory, Pasadena, California 91125, USA*
[b]*Argonne National Laboratory, IPNS Division, Argonne, Illinois 60439, USA*
Email: loeffler@caltech.edu

Small-angle neutron scattering experiments were performed on the bulk amorphous alloy $Zr_{41.2}Ti_{13.8}Cu_{12.5}Ni_{10}Be_{22.5}$ (Vit1®, subscripts indicate at.%) and on other alloys, where the (Zr,Ti) and (Cu,Be) contents were varied by following the line in composition space connecting Vit1 and $Zr_{46.8}Ti_{8.2}Cu_{7.5}Ni_{10}Be_{27.5}$ (Vit4®). The small-angle neutron scattering data of the samples, annealed at temperatures between 603 K and 663 K, show interference peaks, giving evidence for spatially correlated arrangements of inhomogeneities. The Q values of the interference peaks, Q_{max}, decrease with increasing annealing temperature T_a and, at a given annealing temperature, with composition following the connecting line from Vit1 to Vit4. Down to the glass transition temperature T_g, the data follow a relation $1/L^2 \propto (T_s - T_a)$ as predicted by the linearized Cahn theory, with $L = 2\pi/Q_{max}$ the characteristic wavelength of the decomposition and T_s the apparent spinodal temperature. Below T_g, a different behavior is observed, which may be either due to a change in atomic diffusion or due to an insufficient relaxation of the samples.

1. Introduction

Since the first systematic studies on the crystallization behavior in supercooled liquids (Turnbull & Cech, 1950), many investigations have been devoted to the understanding of the thermodynamics and kinetics in various types of liquids (see, e.g., Herlach, 1994). Usually, such experiments are difficult to perform, since, in most alloys, the time scale for crystallization drops very rapidly with undercooling and is experimentally inaccessible at about 0.7 of the melting temperature.

Recently, new multicomponent glass forming systems with a high thermal stability and excellent glass forming ability were found (Drehman & Greer, 1984; Inoue *et al.*, 1990; Zhang *et al.*, 1991; Peker & Johnson, 1993). The critical cooling rate to bypass crystallization and to form a metallic glass is less than 100 K/s in these alloys. This value is several orders of magnitude smaller than the one for monatomic or binary metallic liquids, typically 10^7 to 10^9 K/s. Thus, new 'bulk amorphous alloys' can be produced with a diameter of 1 cm or more in their smallest dimension. Besides possible technical applications, the resistance of the undercooled melt to crystallization in these alloys has opened numerous opportunities to study the glass transition, thermophysical properties, and crystal nucleation kinetics in the undercooled liquid.

One of the best bulk metallic glass formers known so far, with a critical cooling rate of about 1 K/s, is the alloy $Zr_{41.2}Ti_{13.8}Cu_{12.5}Ni_{10}Be_{22.5}$ (Vit1) developed by Peker & Johnson, 1993 (the subscripts in the formula give the concentration of components in at. %). The pathway of crystallization of the glassy alloy has been investigated by small-angle neutron scattering (SANS) after heating it into the supercooled liquid regime. A characteristic maximum of the scattering curves has been found, giving evidence for phase separation in these materials (Schneider *et al.*, 1996; Wiedenmann & Liu, 1996; Schneider *et al.*, 1997; Hermann *et al.*, 1998).

For a detailed understanding of the crystallization pathway in these Zr based bulk amorphous alloys, we have carried out further SANS studies on Vit1 as well as on the alloy $Zr_{46.8}Ti_{8.2}Cu_{7.5}Ni_{10}Be_{27.5}$ (Vit4), also developed by Peker & Johnson (1993). In addition, we have investigated three other compositions which lie along the line in composition space connecting Vit1 and Vit4 (replacing successively Ti by Zr and Cu by Be).

2. Experimental procedure

The 5 alloy compositions were prepared as 25 g ingots by arc melting a mixture of the pure elements (purity > 99.8 %) in a titanium gettered argon atmosphere. The ingots were then remelted in a silica tube with an inner diameter of 10 mm (vacuum $\approx 10^{-5}$ mbar) and subsequently water quenched with a cooling rate of about 10 K/s. From the resulting glassy rods, we cut several disks of 1 mm thickness and annealed them for several hours at temperatures between 593 K and 683 K in a vacuum of 10^{-3} mbar (30 h at 593 K, 603 K; 15 h at 613 K, 623 K, 633 K, 643 K; 1 h at 663 K, 683 K).

The glass transition and crystallization of the as-prepared alloys was studied with a Perkin-Elmer differential scanning calorimeter (DSC 7). The SANS measurements were performed on all as-prepared and annealed samples at the time-of-flight small-angle diffractometer SAD (Thiyagarajan *et al.*, 1997) at the Intense Pulsed Neutron Source at Argonne National Laboratory. By using neutrons of wavelength λ = 1 to 14 Å simultaneously in time-of-flight mode, this instrument produces SANS data in the Q region of 0.006 to 0.3Å^{-1} in a single measurement ($Q = 4\pi \sin\theta/\lambda$, with θ = half the scattering angle).

3. Experimental results

Fig. 1 shows the DSC scans of the alloys Vit1, Vit4, and of the three other alloys which lie along the connecting line by replacing successively Ti by Zr and Cu by Be, further denoted as Vit1A, Vit1B and Vit1C (see also Hays *et al.*, 1999). Within experimental error, all alloys have the same glass transition temperature T_g of about 636 K. However, the crystallization behavior of the alloys is quite different. In Vit1, four crystallization peaks are detected by DSC, with the first crystallization starting at 708 K. In Vit1A, the first crystallization event shifts up to 733 K. This trend is followed in Vit1B, where only one crystallization, starting at 759 K, is detected. Vit1C and Vit4 show two crystallization events, starting at 746 K. Thus, the alloy Vit1B, showing the highest undercooling $\Delta T = T_{x1} - T_g$ = 123 K (with T_{x1} the first crystallization temperature) and only one crystallization event, may be the ideal composition to study the crystallization pathway of multicomponent bulk amorphous alloys.

Fig. 2 shows the SANS intensity data of Vit1, Vit1A and Vit1B annealed at different temperatures. In all three compositions, a clear interference maximum, indicating spatially correlated arrangements of inhomogeneities, is visible up to annealing temperatures of 663 K (Vit1), 643 K (Vit1A) and 633 K (Vit1B). Furthermore, for all three compositions, the SANS intensity peak shifts down to lower Q values with increasing annealing temperature.

For a better comparison of the scattering intensity, Fig. 3 shows the SANS intensity data of all 5 compositions at certain annealing temperatures (603 K to 633 K). With decreasing Ti content, the

interference peak shifts down to lower Q values. After annealing at 603 K, the scattering contrast is the highest for Vit1, but after annealing at higher temperatures, the scattering contrast is higher for Vit1A (T_a = 613 K) and Vit1B (T_a = 623 K, 633 K).

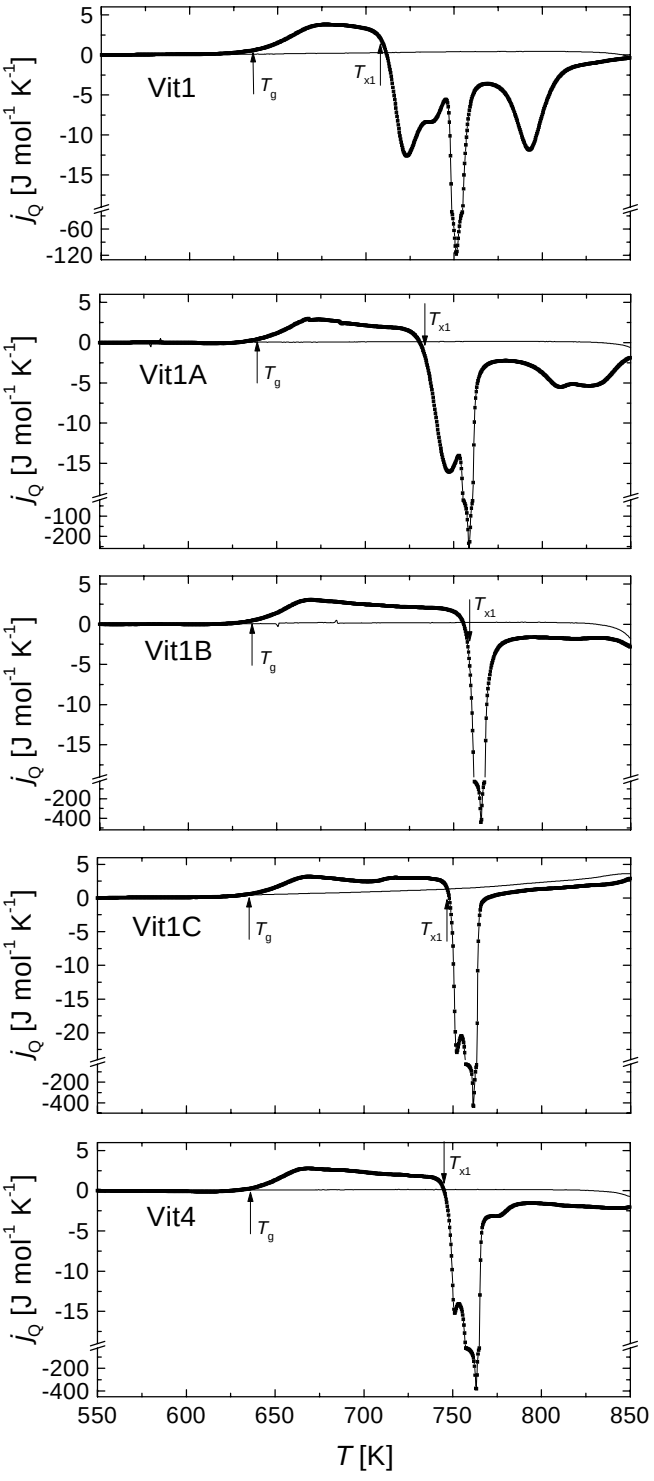

Figure 1
DSC scans of Vit1 ($Zr_{41.2}Ti_{13.8}Cu_{12.5}Ni_{10}Be_{22.5}$), Vit1A ($Zr_{42.6}Ti_{12.4}Cu_{11.25}Ni_{10}Be_{23.75}$), Vit1B ($Zr_{44}Ti_{11}Cu_{10}Ni_{10}Be_{25}$), Vit1C ($Zr_{45.4}Ti_{9.6}Cu_{8.75}Ni_{10}Be_{26.25}$) and Vit4 ($Zr_{46.8}Ti_{8.2}Cu_{7.5}Ni_{10}Be_{27.5}$), performed at a heating rate of 10 K/min (j_Q = endothermic heat flow). The alloy Vit1B shows the highest undercooling $\Delta T = T_{x1} - T_g$.

4. Discussion

In agreement with the results of Schneider *et al.* (1997) and Hermann *et al.* (1998), the SANS data of Vit1 show interference peaks when annealed between 603 K and 663 K (cf. Fig. 2*a*). These interference peaks shift down to lower Q values with increasing annealing temperature T_a. The same trend is also visible in Vit1A and Vit1B (cf. Fig. 2*b* and *c*). Furthermore, at a given annealing temperature, when following the connecting line from Vit1 to Vit4, the interference peaks are shifted down to lower Q values (cf. Fig. 3).

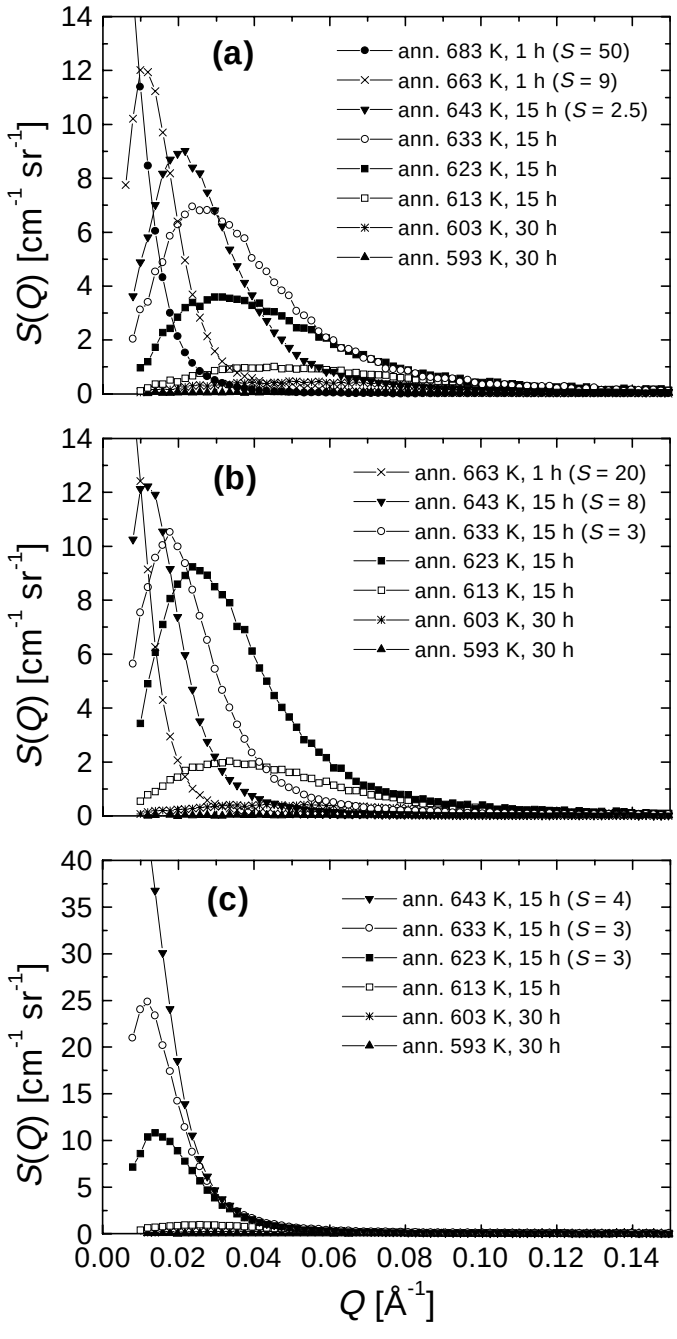

Figure 2
SANS intensity data of (*a*) Vit1, (*b*) Vit1A and (*c*) Vit1B annealed at different temperatures, as indicated in the figure. For a better comparison, the intensity of some samples is reduced by the scaling factor S, given in parentheses.

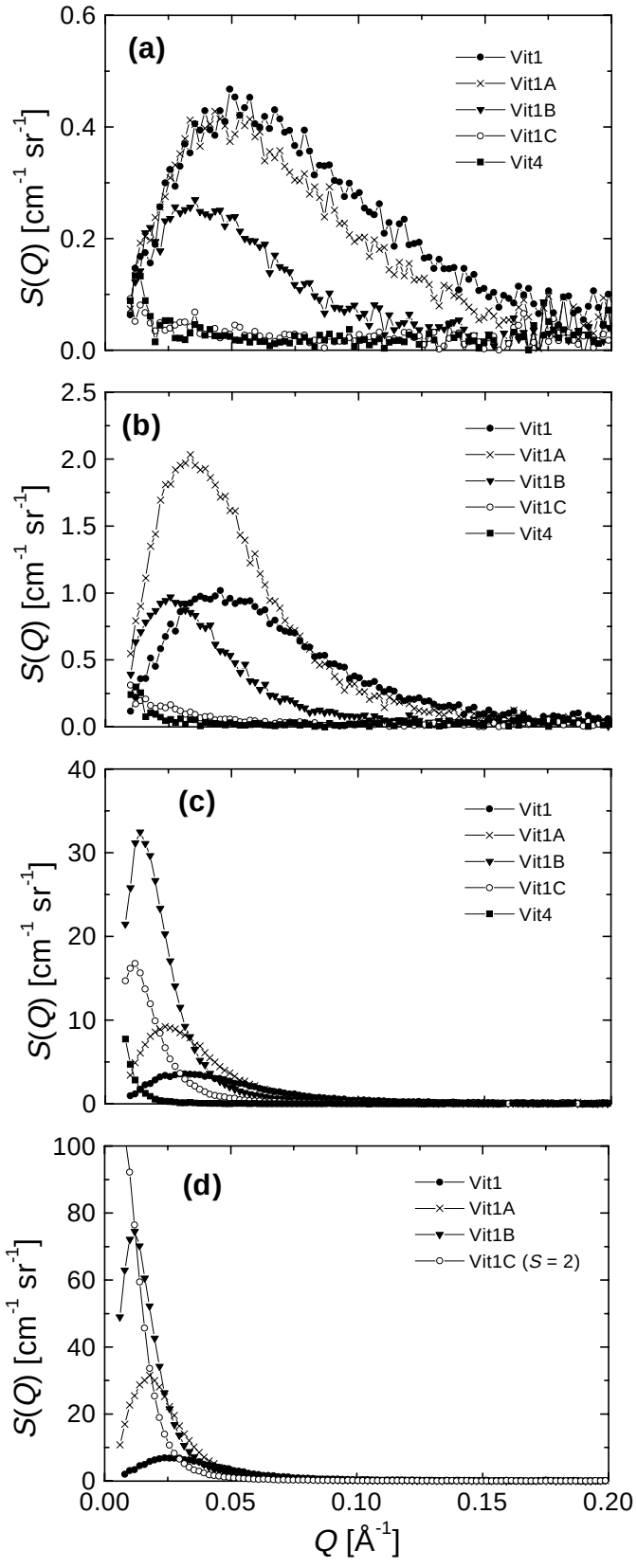

Figure 3
SANS intensity data of all 5 compositions (Vit1, Vit1A to C and Vit4), annealed at (*a*) 603 K, (*b*) 613 K, (*c*) 623 K and (*d*) 633 K. The SANS intensity of Vit1C in Fig. 3*d* is reduced by a factor of 2 ($S = 2$).

In general, the interference peaks give evidence for spatially correlated arrangements of inhomogeneities. Thus, during the annealing process, the supercooled liquid must have decomposed on a fixed length scale into regions with different compositions. At a given annealing temperature, this fixed length scale is different for the different alloys and increases along the connecting line from Vit1 to Vit4.

The high stability against crystallization in these multicomponent alloys may be explained by a model based on this decomposition. With progressive decomposition the local crystal nucleation rate increases drastically, since the composition gets progressively closer to that of the primarily solidified phase. This results in an abrupt onset of crystallization after an incubation time t_0 within one of the decomposed amorphous phases. Since the decomposition initiates the crystallization, the final result (after relaxation) is a crystalline phase embedded in a decomposed amorphous phase, with the size of the crystalline phase related to the length scale of the decomposition.

Indeed, *in-situ* SANS experiments show a temporal evolution of the particle diameter of the crystalline phase, which can be perfectly described by this model (for details, see Löffler & Johnson, 1999). Furthermore, these experiments resolve a small shift of Q_{max} (the Q value at the peak position) with time, giving evidence for simultaneous chemical redistribution and crystal growth in the later stages. In Vit1A, for example, the peak maximum shifts from 0.036 Å^{-1} (after 200 min, where the maximum developed) to 0.026 Å^{-1} (after 600 min), and then Q_{max} stays constant up to a total counting time of 915 min (Löffler *et al.*, 1999).

In the following, we attempt to identify the mechanism of decomposition. This is, however, difficult since the above arguments make clear that decomposition and crystallization cannot be separated. On the other hand, we suggest that the length scale of the decomposition in the early stages determines the intercrystalline spacing in the later stages (after relaxation).

In Cahn's linearized theory of spinodal decomposition (Huston *et al.*, 1966), the characteristic wavelength of the decomposition, L, is proportional to the square root of the ratio of the gradient energy (with respect to composition change) and the curvature of the free energy (Cahn, 1961). The latter depends on $(T_s - T_a)$, with T_s the coherent spinodal temperature and T_a the annealing temperature. The wavelength of the decomposition is inversely proportional to the square root of $(T_s - T_a)$, *i.e.*,

$$\frac{1}{L^2} = \frac{Q_{max}^2}{4\pi^2} \propto T_s - T_a \,. \qquad (1)$$

Fig. 4 shows the values of $1/L^2$ as a function of T_a for all samples investigated. The data follow equation (1) down to an annealing temperature of 623 K and show a change in slope for lower annealing temperatures. Fig. 4 shows straight line fits, according to equation (1), for the experimental data in both regimes. The extrapolation of the fits down to $1/L^2 = 0$, *i.e.*, $L \rightarrow \infty$, gives (in the high temperature regime) apparent values of T_s = 670 K, 649 K and 642 K for the alloys Vit1, Vit1A and Vit1B. In Vit1C, an interference maximum developed only at 623 K and no maximum was detected in Vit4. Presumably, Vit4 also decomposes, but on a length scale which cannot be resolved by SANS. We also performed Auger scanning microscopy experiments on the Vit4 sample, annealed at 623 K, and could not resolve any decomposition down to scales of 1 μm.

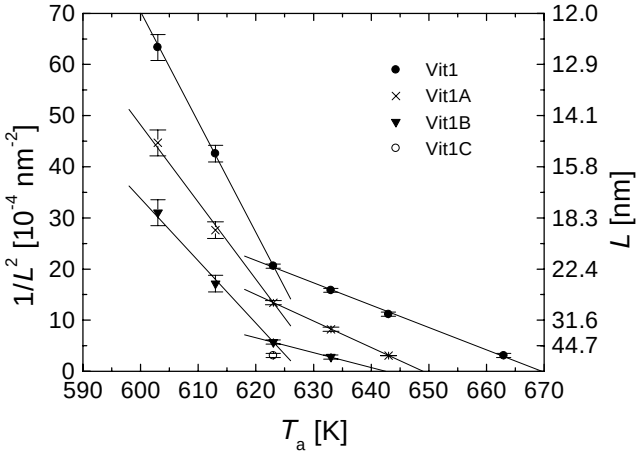

Figure 4
$1/L^2$ vs. T_a plot for the alloys Vit1 and Vit1A to C. Straight lines: fits to the data according to equation (1); the error bars reflect the accuracy in reading the peak maximum.

The crossover in the $1/L^2$ vs. T_a plot occurs at the glass transition temperature T_g = 623 K (T_g depends on the heating rate; therefore, it is lower for the long-time annealed samples than for those measured by DSC, cf. Fig. 1). The crossover in Fig. 4 is in accordance with diffusion experiments performed by Geyer *et al.* (1995), where a crossover of the self-diffusion of Be in Vit1 has been found at the same temperature T_g of 623 K for experiments conducted on roughly the same time scales. The change of decomposition as indicated by Fig. 4 may therefore be explained by a change in diffusion mechanism at T_g, as reported by Geyer *et al.* (1995). On the other hand, the time scale for relaxation increases drastically at temperatures below T_g. Thus, the samples annealed below T_g may not be fully relaxed, in contrast to the samples annealed above 623 K, where 10 h of annealing is sufficient for relaxation. A further relaxation, however, may reduce Q_{max} and lower the value of $1/L^2$ for the low-temperature annealed samples, providing an alternative explanation for the crossover behavior. Further SANS experiments are under way which involve investigating the relaxation behavior at temperatures below T_g on longer time scales.

5. Conclusions

We have presented DSC and SANS measurements on the bulk amorphous alloys $Zr_{41.2}Ti_{13.8}Cu_{12.5}Ni_{10}Be_{22.5}$ (Vit1) and $Zr_{46.8}Ti_{8.2}Cu_{7.5}Ni_{10}Be_{27.5}$ (Vit4) as well as on three other alloys along the connecting line in composition space by varying the (Zr,Ti) and (Cu,Be) concentrations (Vit1A, B and C). At a heating rate of 10 K/min, all alloys show a glass transition temperature of around 636 K. The crystallization behavior, however, varies significantly for the different compositions, with the highest undercooling, T_{x1} - T_g, for the alloy Vit1B.

The SANS data of the alloys annealed between 603 K and 663 K show interference peaks, giving evidence for spatially correlated arrangements of inhomogeneities. The wavelength of these correlations, L, increases with increasing annealing temperature and, at a given annealing temperature, with composition following the connecting line from Vit1 to Vit4. The wavelength follows a relation $1/L^2 \propto (T_s - T_a)$ as predicted by Cahn's theory in two distinguishable regimes, with a crossover in slope at the glass transition temperature T_g = 623 K. This crossover occurs either owing to a change in diffusion mechanism at T_g as reported in the literature or due to an insufficient relaxation of the low-temperature annealed samples. The interference maxima of the different compositions occur up to annealing temperatures T_a = 670 K (in Vit1), 649 K (Vit1A), 642 K (Vit1B) and 623 K (Vit1C). No interference maximum was observed in Vit4.

The authors acknowledge the assistance of Ed Lang while running the SANS experiment. This work was supported by the U.S. Department of Energy (Grant No. DEFG-03-86ER45242) and benefited from the use of the Intense Pulsed Neutron Source, funded by the U. S. Department of Energy, Office of Basic Energy Sciences under contract W-31-109-ENG-38 to the University of Chicago. Partial support for J. Löffler was provided by the Alexander von Humboldt Foundation via the Feodor Lynen Program.

References

Cahn, J. W. (1961). *Acta Metall.*, **9**, 795 – 801.
Drehman, A. J. & Greer, A.L. (1984). *Acta Metall.*, **32**, 323 – 332.
Geyer, U., Schneider, S., Johnson, W. L., Qiu, Y., Tombrello, T. A. & Macht, M.-P. (1995). *Phys. Rev. Lett.*, **75**, 2364 – 2367.
Hays, C. C., Kim, C. P. & Johnson, W. L. (1999). *Appl. Phys. Lett.*, **75**, 1089 – 1091.
Herlach, D. M. (1994). *Mater. Sci. Eng.*, **R12**, 177 – 272 and references therein.
Hermann H., Wiedenmann A. & Uebele P. (1998). *Physica B*, **241 – 243**, 352 – 354.
Huston, E. L., Cahn, J. W. & Hilliard, J. E. (1966). *Acta Metall.*, **14**, 1053 – 1062.
Inoue, A., Zhang, T. & Masumoto, T. (1990). *Mater. Trans. JIM*, **31**, 425 – 428.
Löffler, J. F. & Johnson, W. L. (1999). *Mater. Sci. Eng.*, submitted.
Löffler, J. F., Johnson, W. L., Wagner, W. & Thiyagarajan, P. (1999). *Mater. Sci. Forum*, in press.
Peker, A. & Johnson, W. L. (1993). *Appl. Phys. Lett.*, **63**, 2342 – 2344.
Schneider, S., Thiyagarajan, P. & Johnson, W. L. (1996). *Appl. Phys. Lett.*, **68**, 493 – 495.
Schneider, S., Geyer, U., Thiyagarajan, P. & Johnson, W. L. (1997). *Mater. Sci. Forum*, **235 – 238**, 337 – 342.
Thiyagarajan, P., Epperson, J. E., Crawford, R. K., Carpenter, J. M., Klippert, T.E. & Wozniak, D. G. (1997). *J. Appl. Cryst.*, **30**, 280 – 293.
Turnbull, D. & Cech R. E. (1950). *J. Appl. Phys.*, **21**, 804 – 810.
Wiedenmann, A. & Liu, Jun-Ming (1996). *Solid State Comm.*, **100**, 331 – 335.
Zhang, T., Inoue, A. & Masumoto, T. (1991). *Mater. Trans. JIM*, **32**, 1005 – 1010.

 Received 12 June 1999 • Accepted 18 November 1999